

Geophysical Research Letters



RESEARCH LETTER

10.1029/2019GL082208

Key Points:

- The high-salinity core observed in the Bay of Bengal during the southwest monsoon originates from the western equatorial Indian Ocean
- The Somali Current, Equatorial Undercurrent, and Monsoon Current are key to supply and variability of the Bay of Bengal high-salinity core
- Wind stress and El Niño determine the Equatorial Undercurrent velocity and thus the strength of the high-salinity core on interannual scales

Supporting Information:

- Supporting Information S1

Correspondence to:

A. Sanchez-Franks,
alsf@noc.ac.uk

Citation:

Sanchez-Franks, A., Webber, B. G. M., King, B. A., Vinayachandran, P. N., Matthews, A. J., Sheehan, P. M. F., et al. (2019). The railroad switch effect of seasonally reversing currents on the Bay of Bengal high-salinity core. *Geophysical Research Letters*, 46. <https://doi.org/10.1029/2019GL082208>

Received 29 JAN 2019

Accepted 6 MAY 2019

Accepted article online 8 MAY 2019

The Railroad Switch Effect of Seasonally Reversing Currents on the Bay of Bengal High-Salinity Core

A. Sanchez-Franks¹ , B. G. M. Webber^{2,3} , B. A. King¹ , P. N. Vinayachandran⁴ , A. J. Matthews^{2,5} , P. M. F. Sheehan² , A. Behara⁴, and C. P. Neema⁴

¹National Oceanography Centre, Southampton, UK, ²Centre for Ocean and Atmospheric Sciences, School of Environmental Sciences, University of East Anglia, Norwich, UK, ³Climatic Research Unit, University of East Anglia, Norwich, UK, ⁴Centre for Atmospheric and Oceanic Sciences, Indian Institute of Science, Bangalore, India, ⁵School of Mathematics, University of East Anglia, Norwich, UK

Abstract The Southwest Monsoon Current (SMC) flows eastward from the Arabian Sea into the Bay of Bengal (BoB) during summer, advecting a core of high-salinity water. This high-salinity core has been linked with Arabian Sea High-Salinity Water that is presumed to enter the BoB directly from the Arabian Sea via the SMC. Here we show that the high-salinity core originates primarily from the western equatorial Indian Ocean, reaching the BoB via the Somali Current, the Equatorial Undercurrent, and the SMC. Years with anomalously saline high-salinity cores are linked with the East Africa Coastal Current and the Somali Current winter convergence and an anomalously strong Equatorial Undercurrent. Seasonal reversals that occur at the Somali Current and SMC junctions act as railroad switches diverting water masses to different basins in the northern Indian Ocean. Interannual fluctuations of the Equatorial Undercurrent are linked to wind stress and El Niño.

Plain Language Summary The northern Indian Ocean experiences a seasonal reversal of currents due to monsoon winds. During the summer, the monsoon current transports high-salinity water from the Arabian Sea into the Bay of Bengal. This supply of salty water is believed to originate from the eastern Arabian Sea. Here we find that the intrusion of high-salinity water originates instead from the western Arabian Sea. The origins of the high-salinity water are traced to the western equatorial Indian Ocean via a seasonal equatorial undercurrent. In the western equatorial Indian Ocean there is a seasonal convergence of currents that is crucial to the supply of this salty water. Variability in the equatorial undercurrent is linked to wind fields and the El Niño–Southern Oscillation. As a result, these findings shed new insight into which large-scale patterns influence the subsurface salinity in the Bay of Bengal that then modulate the variability of sea surface temperature and the strength of air-sea coupling in this region. Better representation of interaction between patterns of climate variability and the currents of the equatorial Indian Ocean could improve the representation of the Bay of Bengal in climate models and thus the representation of monsoon processes, including rainfall.

1. Introduction

One of the most remarkable characteristics of the northern Indian Ocean, which distinguishes it from any other ocean basin in the world, is the seasonal reversal of its major current systems. The South Asian monsoon dominates temporal variability of the surface circulation, leading to the reversal of the currents (Goswami, 2005; Shankar et al., 2002). In the western northern Indian Ocean, the Arabian Sea hosts the Somali Current that flows southward in boreal winter and northward in boreal summer (Schott & McCreary, 2001). In the eastern northern Indian Ocean, the Bay of Bengal (BoB) is connected to the Arabian Sea via the Northeast Monsoon Current that flows westward from the BoB to the Arabian Sea during winter and via the Southwest Monsoon Current (SMC) that flows eastward from the Arabian Sea to the BoB during summer (Schott & McCreary, 2001). The monsoon currents can have a large impact on the distribution of northern Indian Ocean salinity (Vinayachandran et al., 1999, 2013), which increases from east (i.e., BoB) to west (i.e., Arabian Sea). The Arabian Sea surface waters are highly saline due to strong evaporation (Antonov et al., 2010; Chatterjee et al., 2012), whereas the BoB is comparatively fresh at the surface due to the outflow from the Ganges-Brahmaputra and other river systems and monsoon rainfall (Shetye et al., 1996; Vinayachandran et al., 2002).

©2019. The Authors.

This is an open access article under the terms of the Creative Commons Attribution License, which permits use, distribution and reproduction in any medium, provided the original work is properly cited.

One of the key features of the SMC is a core of high-salinity water it advects into the BoB (Murty et al., 1992; Vinayachandran et al., 2013). The high-salinity core (HSC) plays an important role in maintaining the BoB's salinity balance, as it is the main source of salinity available to balance the BoB's net outflow of freshwater (Schott et al., 2009; Vinayachandran et al., 1999, 2013). To date, several studies have linked the HSC to Arabian Sea High-Salinity Water (ASHSW), which originates from the northern Arabian Sea and is transported to the BoB via the SMC (Jensen, 2001; Jensen et al., 2016; Schott & McCreary, 2001; Vinayachandran et al., 1999; Webber et al., 2018).

Indian Ocean equatorial currents are also subject to the seasonal influence of the monsoon winds. Surface and subsurface eastward flowing currents form, within the upper thermocline, along the Indian Ocean equator during the intermonsoon periods (Schott & McCreary, 2001; Wyrski, 1973). At the surface, the narrow eastward current is known as the Wyrski Jet (Wyrski, 1973), and below it lies the Indian Ocean Equatorial Undercurrent (EUC; Knauss & Taft, 1964; Nagura & McPhaden, 2016; Reppin et al., 1999; Schott & McCreary, 2001). The equatorial currents connect the western and eastern parts of the equatorial Indian Ocean and can have major impacts on the transport and distribution of ocean heat (Reverdin, 1987; Wyrski, 1973). In this study, we focus on the subsurface current, the EUC, and demonstrate for the first time a connection between the EUC and the BoB HSC. A new paradigm is presented to explain the source, pathways, and variability of the BoB HSC. Driving mechanisms for fluctuations of the EUC and BoB HSC on interannual time scales are also explored.

2. Data and Methods

For this study, the Nucleus for European Modelling of the Ocean (NEMO) version 3.1 (Madec, 2008) estimates of velocity and salinity were used. NEMO is a global ocean model (analysis and forecasting system) with a resolution of $1/12^\circ$ in the horizontal and 50 levels in the vertical, with 1-m resolution at the surface, increasing to 450 m near the bottom (5,500 m). Surface forcing is from operational forecasts of the European Centre for Medium-Range Weather Forecasts. NEMO assimilates a combination of observational data sets (satellite and in situ).

NEMO was compared with a product constructed from optimally interpolated (OI) profiles of Argo floats. The OI mapping is constructed based on anomalies relative to a reference ocean, from the monthly World Ocean Atlas climatology (Boyer et al., 2013). Data are gridded at 25 longitude grid points at 0.5° intervals, and days are centered on midnight universal time coordinated with a window of ± 0.5 days. More details on this product and the method are described in Desbruyeres et al. (2017).

The wind field is investigated using TropFlux zonal wind stress (Kumar et al., 2012). In the tropical Indian Ocean, a region of sparse data and large model biases, TropFlux has been shown to outperform other reanalysis products (Sanchez-Franks et al., 2018). The Indian Ocean Dipole (IOD) is quantified as the difference between sea surface temperature (SST) anomalies in the western ($50\text{--}70^\circ\text{E}$, 10°S to 10°N) and eastern ($90\text{--}110^\circ\text{E}$, 10°S to 0°N) equatorial Indian Ocean (Saji et al., 1999). Weekly values of the Dipole Mode Index and the oceanic Niño3.4 El Niño index (the SST anomaly for the region: 5°N to 5°S and $170\text{--}120^\circ\text{W}$) are interpolated to daily resolution for comparison with the NEMO daily product. Both indices are based on the weekly updated Reynolds OIv2 SST analysis (Reynolds et al., 2002).

All data have daily resolution (or interpolated to daily resolution where needed) for the years 2007 to 2016, and a 61-day smoothing has been applied to all variables to reduce noise associated with high-frequency variability.

3. The BoB HSC

The NEMO subsurface salinity anomalies along 7°N show the HSC as a recurring annual feature with positive salinity anomalies appearing during boreal summer (Figure 1a). Very high-salinity anomalies (≥ 0.15), representative of an unusually strong HSC, are observed during the summers of 2007, 2014, and 2016 and to a lesser extent during 2012 and 2013 (Figure 1a). Zero or negative salinity anomalies are observed during the summers of 2010 and 2015 (Figure 1a). The structure of the subsurface (90–130 m) salinity across the wider BoB during the summer of 2014 (Figure 1b) shows the intrusion of a high-salinity tongue alongside the eastward flowing SMC (surface current vectors from OSCAR; Bonjean & Lagerloef, 2002), in agreement with Vinayachandran et al. (2013, 2018) and Webber et al. (2018). The SMC is a surface-intensified current

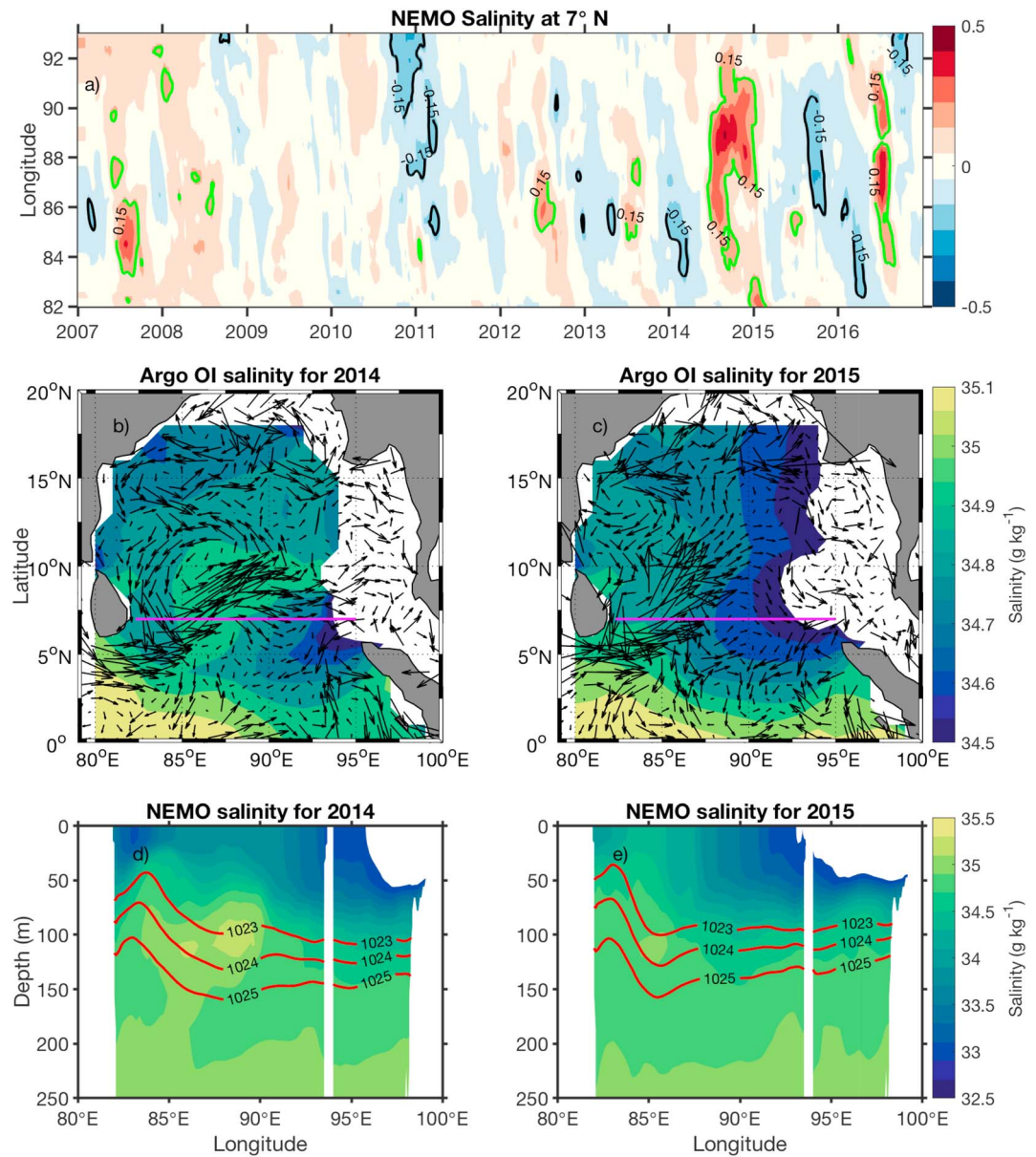


Figure 1. Salinity in the Bay of Bengal at 7°N for (a) NEMO subsurface (110–130 m) salinity anomalies (from long-term mean) with 61-day smoothing applied from 2007 to 2016. (b) OSCAR surface current velocities (vector) and Argo optimally interpolated (OI) subsurface (110–130 m) salinity (shaded) during anomalously high high-salinity core (HSC) summer (July, August, September) 2014 and (c) anomalously low HSC summer 2015. (d) NEMO vertical cross sections of salinity at 7°N during anomalously high HSC summer 2014 and (e) anomalously low HSC summer 2015. Magenta line (b, c) indicates location of vertical cross section. Red lines (d, e) indicate the location of the 1,023-, 1,024-, and 1,025-kg/m³ isopycnal. NEMO = Nucleus for European Modelling of the Ocean.

with northward flow extending to a depth of 300 m (Vinayachandran et al., 2018; Webber et al., 2018). As the HSC is advected north by the SMC, it is subducted under the fresher, lighter waters of the northern BoB (Vinayachandran et al., 1999, 2013). Changes to the HSC may also occur from the surface flows of saline waters being subducted (Vinayachandran et al., 2013).

A comparison of the cross sections of the vertical structure of salinity at 7°N from NEMO (Figures 1d and 1e) and the Argo OI (not shown) show that the model agrees well with the observations. Both NEMO (Figure 1d) and the Argo OI show the structure of the HSC (>35 g/kg) centered between 75 and 130 m and 85–90°E for summer 2014 (Figure 1d) and 83–87°E for the summer of 2015 (Figure 1e), consistent with previous studies (Vinayachandran et al., 2013; Webber et al., 2018). Webber et al. (2018) found that the NEMO ocean model

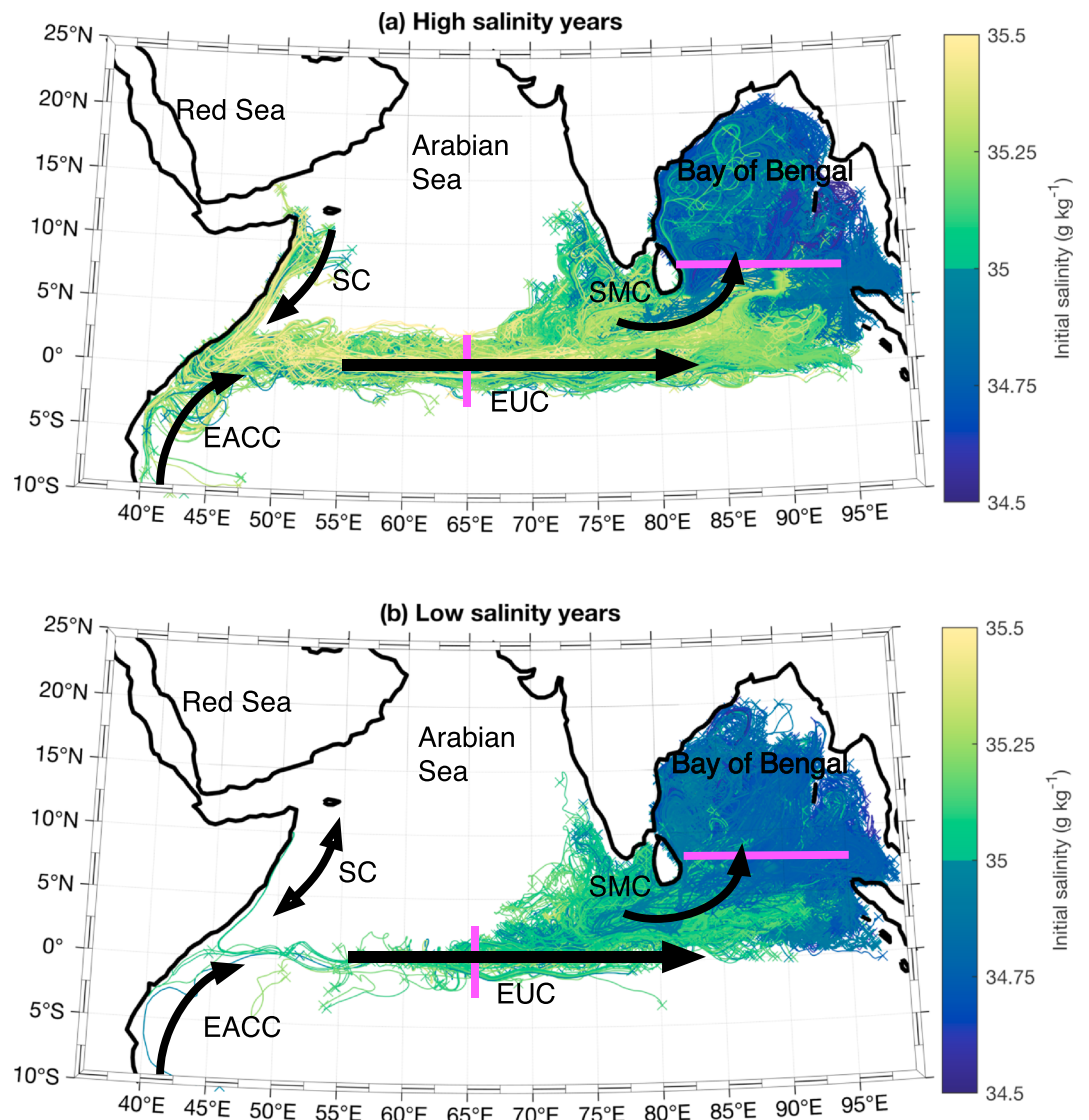


Figure 2. Composite of Nucleus for European Modelling of the Ocean salinity particles released at 82–90°E, 7°N at 5-day intervals from 1 June to 30 August and tracked backward to 1 January for high-salinity years (2007, 2014, and 2016) and low-salinity years (2008, 2010, and 2015) on the 1,024-kg/m³ isopycnal. Magenta lines indicate regions where the Equatorial Undercurrent (EUC) and the Bay of Bengal high-salinity core were measured. SC = Somali Current; EACC = East African Coastal Current; SMC = Southwest Monsoon Current.

provides an accurate representation of the velocity, salinity, and density structure in the BoB, compared to observations made during the 2016 monsoon season that were not assimilated into the model (Figure 2 of Webber et al., 2018). We note that NEMO shows a more defined salinity core structure and higher values for the HSC than the Argo OI. This can primarily be attributed to the low spatial and temporal resolution of the Argo OI product.

The HSC is a pervasive feature in the southern BoB that occurs alongside the SMC. We note that the relationship between the strength of the SMC and variability in the HSC appears weak (Figure S1 in the supporting information). Spatial variability of the HSC is large (Figure 1a), and changes in isopycnal depth (heave) are substantial. The salinity core typically rests on the 1,024-kg/m³ isopycnal (Figures 1d and 1e), which is within the known density range (1,022.8–1,024 kg/m³) for the ASHSW (Shenoi et al., 1993). Therefore, model salinity and velocity are mapped onto the 1,024-kg m³ isopycnal to trace the pathways of this water mass.

4. The Western Equatorial Indian Ocean Origins of the HSC

To trace the origins of the HSC, a backward trajectory particle experiment was conducted. NEMO velocities were interpolated to the $1,024\text{-kg/m}^3$ isopycnal surface (approximately 80- to 100-m depth across most of the Indian Ocean [Figure S2]). Particles were then tracked backward in time along this surface, neglecting diapycnal diffusivity, which we assume would have a small impact on the backward trajectories on time periods less than 1 year. Model velocities on this isopycnal surface were bilinearly interpolated to the particle locations, and the particles were advected using a fourth-order Runge-Kutta scheme with a time step of 1 hr. This time step is chosen to avoid particles crossing multiple grid boxes within a single time step. To track the origin of water masses that passes through 7°N during the southwest monsoon, particles are released at 5-day intervals from 1 June to 30 August along 7°N (between 82°E and 90°E) and are tracked backward to 1 January. This experiment is repeated for anomalously high/low HSC at 7°N (see below). Similar backward tracking experiments have been shown in Jensen (2003).

Figure 2 shows that during anomalously high-salinity years (2007, 2014, and 2016), highly saline ($>35\text{ g/kg}$) particles predominantly originate from the western equatorial Indian Ocean via the equatorial current and the Somali Current to the north and, to a lesser extent, the East African Coastal Current (EACC) to the south, whereas fresher ($<35\text{ g/kg}$) particles originate from interior BoB recirculation (Figure 2a). The main source of high salinity in the western equatorial Indian Ocean, consistent with Figure 2a, is the Somali Current. Note that the color of each line only represents the salinity of the particle along 7°N and does not account for any change in salinity along the track. During winter the southward Somali Current advects highly saline ($>36\text{ g/kg}$) waters from the western Arabian Sea (Antonov et al., 2010; Chatterjee et al., 2012; Kumar & Prasad, 1999), converges with the EACC, and feeds into the eastward equatorial currents (Schott & McCreary, 2001). During the summer monsoon, however, the Somali Current flows north, diverting the waters from the EACC toward the Arabian Sea and away from the equatorial currents (Wyrtki, 1973). The 8-month time period observed for the anomalously saline HSC particles initialized in July–August in the BoB places their origins in the western Indian Ocean in winter of the previous year. This suggests that the high-salinity water originates from the EACC and Somali Current confluence zone that occurs in winter (Figure 2a). Given that ASHSW is in the $1,022.8\text{--}1,024\text{-kg/m}^3$ density range (Shenoi et al., 1993) and that anticyclonic circulation advects the ASHSW from the northern to the southwestern Arabian Sea (Prasad & Ikeda, 2002), it is likely that some of the source water mass is ASHSW.

Conversely, during the anomalously fresh HSC years (2008, 2010, and 2015), there are significantly fewer high-salinity ($>35\text{ g/kg}$) particles and fewer trajectories along the equator (Figure 2b). In the space of 6–8 months most particles only travel eastward from 55°E (Figure 2b); it takes over 1 year for them to be traced back to the western equatorial Indian Ocean (not shown), suggesting that they would have originated from the western equatorial Indian Ocean during the previous summer, when the Somali Current was flowing north. Composites of velocity on the $1,024\text{-kg/m}^3$ isopycnal surface show that the velocity of the equatorial currents is significantly higher during the anomalously saline HSC years compared with the anomalously fresh HSC years (Figure S2). Slower advection would also allow a longer period for isopycnal mixing to further reduce salinity. At the western boundary instabilities generated by the southern gyre (Kindle & Thompson, 1989) may also contribute to strong water mass mixing.

Sensitivity tests for density class choice and a forward trajectory experiment were also run. The sensitivity test for density class was run using the backward trajectory particle experiment for $1,023\text{-}$ and $1,025\text{-kg/m}^3$ isopycnals. Compared to $1,024\text{-kg/m}^3$ run, both runs show significantly fewer particles originating from the western Arabian Sea (i.e., via the Somali Current; Figure S3). The run for $1,023\text{-kg/m}^3$ surface also suggests that more particles originate from the eastern Arabian Sea for water masses lighter than the HSC (Figures S3, 1d, and 1e). The forward trajectory particle experiment was initiated from a section between 50°E and 55°E along 10°N in the western Arabian Sea every 5 days from 1 December the previous year to 30 January the current year and then run forward until 30 August (Figure S4). This run confirmed that during the high-salinity years, a large number of particles from the western Arabian Sea reached the BoB (Figure S4a), particularly in contrast to the low-salinity years (Figure S4b).

These results suggest the following key points: (1) Most of the HSC water originates from the western equatorial Indian Ocean and the western Arabian Sea is an important source region, (2) the HSC is more likely related to the pathways of the currents rather than transformation or changing properties in the source region, and (3) the existence of an anomalously saline HSC is linked to the equatorial currents velocity

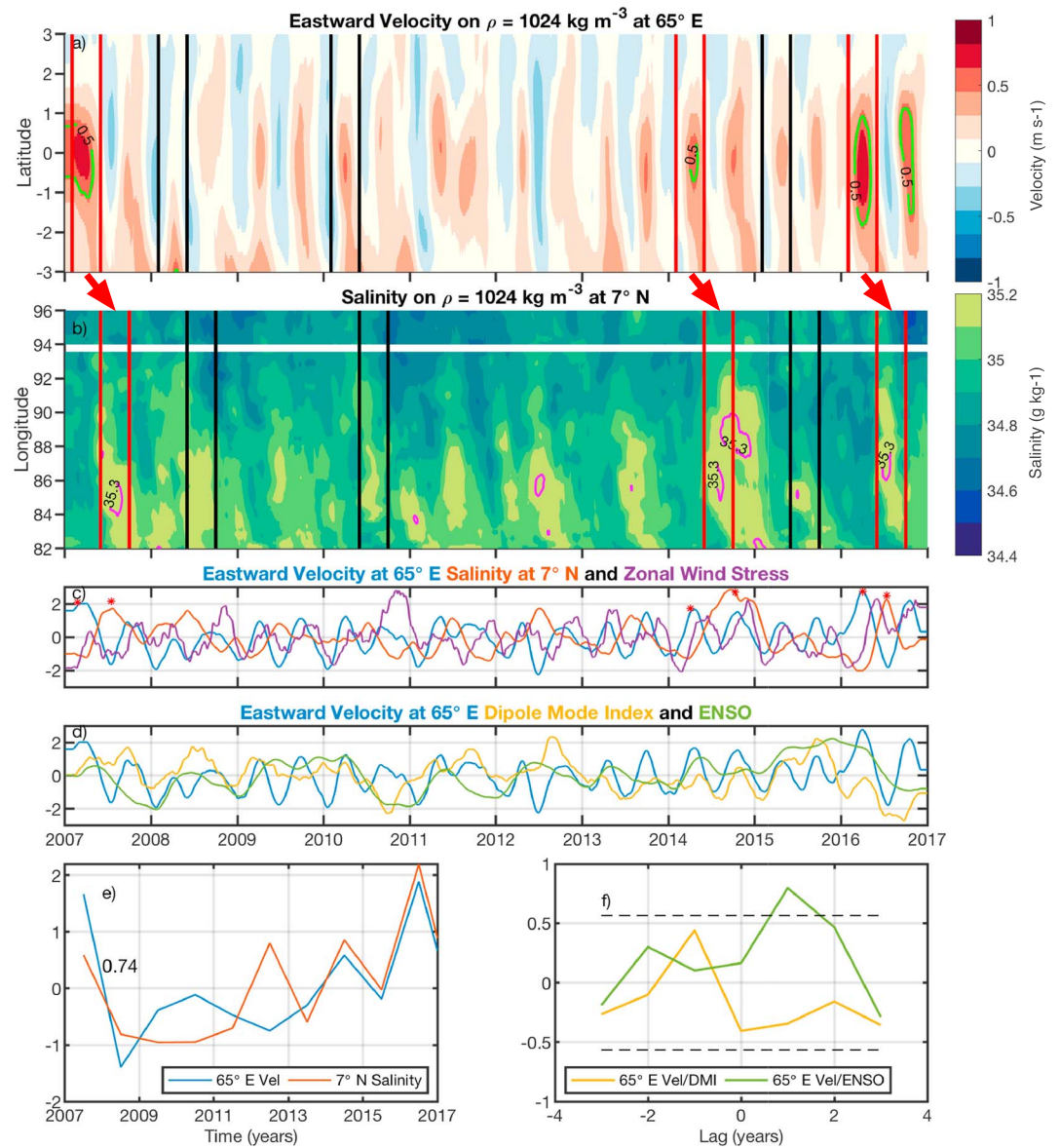


Figure 3. (a) Nucleus for European Modelling of the Ocean eastward velocity (m/s) at 65°E and (b) salinity (g/kg) at 7°N. (c) Eastward velocity at 65°E averaged over 2°S to 1.5°N (blue line), salinity at 7°N averaged over 82°E to 96°E (orange line) and TropFlux zonal wind stress averaged over 2°S to 2°N and 60–90°E (purple line). (d) Eastward velocity at 65°E (blue line), the Dipole Mode Index (DMI; yellow line) and El Niño–Southern Oscillation (ENSO; green line). (e) Annual average of the spring (February–May) eastward velocity at 65°E (blue line) and the summer (June–August) salinity at 7°N (orange line). (f) Lag correlation plots of eastward velocity at 65°E and DMI (yellow line) and eastward velocity at 65°E and ENSO (green line), where positive values indicate DMI and ENSO lead eastward velocity 65°E, and dashed lines represent statistical significance at the 95% level. All data sets have been smoothed with a 61-day moving average, and time series are normalized by their standard deviation.

required to transport highly saline waters from the winter western Indian Ocean convergence zone in the time for the BoB summer monsoon.

5. Variability and Mechanisms for the HSC and the Equatorial Currents

The connection between the HSC in the BoB at 7°N and the equatorial currents is investigated through analysis of NEMO currents and salinity from a section along 65°E between 2°S and 1.5°N (Figure 2; magenta line perpendicular to the equator). The eastward velocity of the equatorial current is centered subsurface (50–130 m) around the equator and experiences a biannual strengthening in speed (Figures 3a and S5),

associated with the spring (February–April) and fall (September) EUC generated from the intermonsoon wind regimes (Chen et al., 2015; Knauss & Taft, 1964; Nagura & McPhaden, 2016; Reppin et al., 1999). On average, the simulated speeds of the EUC appear to be 0.5 m/s during their peak in the spring season (Figure S5), in agreement with observations shown in Nagura and McPhaden (2016). This spring peak is associated with a climatological subsurface salinity maximum (Figure S5). Anomalously high speeds (>0.5 m/s) peaking at the $1,024\text{-kg/m}^3$ isopycnal are observed during the spring (February–April) intermonsoon periods of 2007, 2014, and 2016 at 65°E (Figure 3a; green contour lines and red bars) in agreement with the years with anomalously saline HSC in the BoB (sections 3 and 4). Similarly, anomalously high salinity (>35.2 g/kg) is observed a few months later (June–September) between 83°E and 90°E in the southern BoB (7°N) for the same years (Figure 3b; magenta contour lines and red bars). Years flagged as anomalously low for salinity in the BoB (2008, 2010, and 2015; see Figures 1 and 2) show comparatively weaker eastward velocities and corresponding lower salinity in the southern BoB (Figures 3a and 3b).

Comparison of the eastward velocity at 65°E and the salinity at 7°N clearly shows that peaks in BoB salinity are preceded (by a few months) by a peak in eastward velocity at 65°E , associated with an anomalously strong spring EUC (Figure 3c). Further, the annually averaged spring EUC (fall EUC is excluded as it has no bearing on the summer BoB salinity) compared with the summer (June–August) BoB salinity shows a correlation of 0.74 significant at the 95% level (Figure 3e). Notable exceptions occur during 2012, when a peak in salinity was not accompanied by a peak in EUC velocity (Figure 3e). The higher salinity apparent during that year may have originated from the eastern Arabian Sea, or it may have been a result of higher salinity particles that accumulated in the eastern equatorial Indian Ocean the year before. In general, a strong spring EUC transports the highly saline waters of the winter EACC/Somali Current convergence zone in time for the SMC to advect an anomalously saline HSC into the BoB.

To investigate the mechanisms driving variability in EUC velocity, we examine the equatorial zonal wind stress, the IOD, and the El Niño–Southern Oscillation (ENSO). First, the wind stress is examined as the EUC has been shown to be a response to the intermonsoon wind regimes and in particular to the zonal wind stress along the equator (Chen et al., 2015; Nagura & McPhaden, 2010, 2016). Here, TropFlux Zonal Wind stress is averaged over 2°S to 2°N and 60°E to 90°E . The EUC also has a connection with the IOD (Chen et al., 2015; Zhang et al., 2014), where positive (negative) IOD events represent warm SST anomalies in the western (eastern) Indian Ocean (Yamagata et al., 2004).

Wind stress, the IOD, and ENSO are compared with the eastward velocity at 65°E . All three parameters experience similar biannual variability (Figures 3c and 3d). A lag correlation shows that zonal wind stress leads EUC eastward velocity by 62 days ($r = -0.63$, $p < 0.05$) suggesting that decreases (increases) in easterly winds results in the strengthening (weakening) of the EUC eastward velocity. To investigate the link between the EUC and the IOD and ENSO, all three parameters were annually averaged. ENSO leads EUC variability by 1 year ($r = 0.79$, $p < 0.05$; Figure 3f). In contrast, the link between the IOD and the EUC velocity is not as robust ($r = -0.40$, $p < 0.20$). In general, positive (negative) ENSO results in the strengthening (weakening) of the EUC eastward velocity. It is somewhat surprising that ENSO rather than the IOD dominates the variability of the velocity at 65°E , as the IOD has been shown to dominate the equatorial Indian Ocean (Yu et al., 2005). It is possible that the discrepancy lies in the selected region at 65°E , which is a bit further west of the centers of action depicted in Yu et al. (2005). We also note that 2007 and 2014–2016 were El Niño years.

6. The Railroad Switch Effect of the Indian Ocean's Seasonally Reversing Currents

We have shown thus far that the inflow of high-salinity water into the BoB has its origins in the western equatorial Indian Ocean and that water mass pathways are the key drivers of changes in the BoB's HSC (sections 4 and 5). Results presented here have also underlined the importance of the seasonal reversals of the Somali Current, the SMC, and the EUC as key players on pathways and terminus of high-salinity particles originating from the western Indian Ocean. Based on this, we postulate that there are two key junctions in the water mass pathways: one in the west with the EACC and the Somali Current and another just south of Sri Lanka with the EUC and the Monsoon Current. Depending on the time of year, the current reversals that occur at these junctions act as railroad switches (or points on the British railway system) diverting water masses to different destinations in the northern Indian Ocean. Here, we outline the four such possible

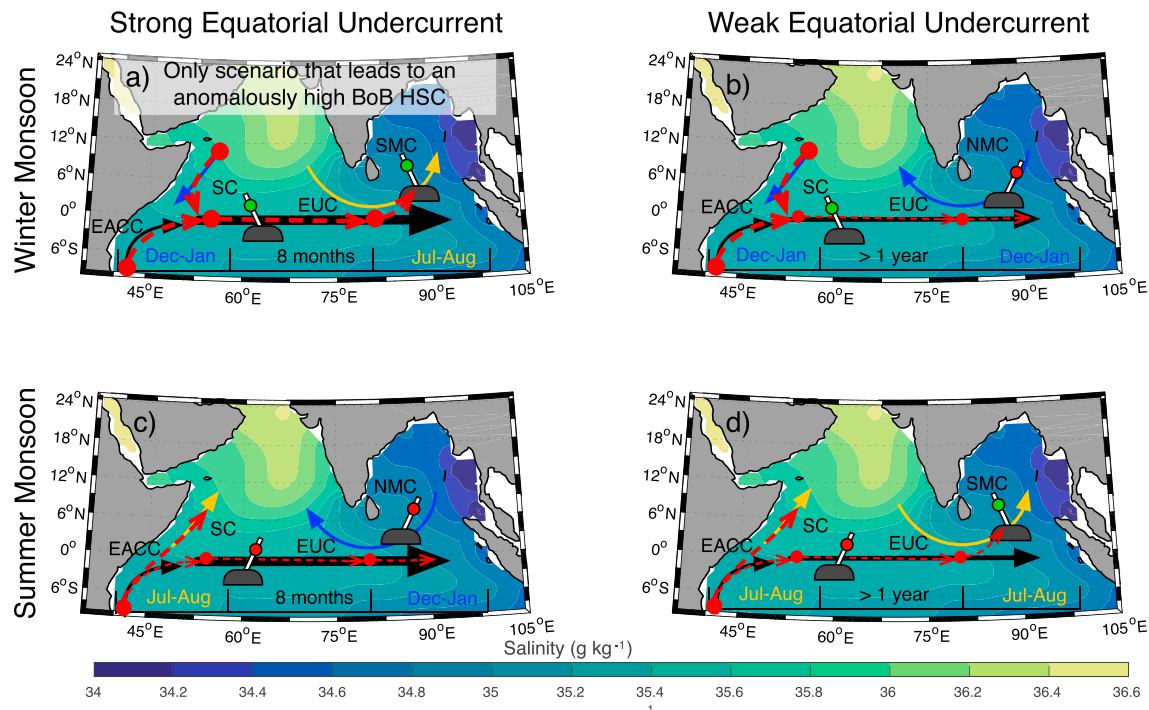


Figure 4. Railroad Switch schematic on subsurface (90 m) salinity climatology (psu; shaded) from the Argo optimally interpolated product for the four Equatorial Undercurrent scenarios: (a, b) winter monsoon and strong (weak) Equatorial Undercurrent and (c, d) summer monsoon and strong (weak) Equatorial Undercurrent. Red dashed arrows indicate high-salinity advection. BoB = Bay of Bengal; HSC = high-salinity core; SMC = Southwest Monsoon Current; SC = Somali Current; EUC = Equatorial Undercurrent; EACC = East African Coastal Current.

railroad track circulation scenarios and the resulting impact on salinity distribution across the northern Indian Ocean and in particular the BoB.

In boreal winter, the Somali Current flows south advecting the highly saline waters of the western Arabian Sea toward the northward flowing EACC feeding into the South Equatorial Counter Current (Schott et al., 2009) and (eventually) the springtime EUC (Figures 4a, 4b, and S6a). During the spring intermonsoon period (February–April), the EUC forms and transports waters from the west to the east equatorial Indian Ocean (Chen et al., 2015; Figure S6b and S6c). Section 4 showed that when the EUC is anomalously strong, the time it takes to advect waters from the western to the eastern equatorial Indian Ocean is approximately 8 months (Figure 2). Hence, for a strong spring EUC, highly saline waters from the wintertime EACC and Somali Current convergence zone reach the eastern equatorial Indian Ocean in time to make the connection with the eastward flowing SMC, which advects those highly saline waters into the BoB (Figures 4a, S6a, S6b, and S6d). Conversely, if the EUC is not anomalously strong, it may take over a year for the highly saline waters of the winter EACC and the Somali Current convergence zone to reach the BoB (Figures 4b, S6c, and S6e). By then, isopycnal mixing may have diluted the waters and the SMC will have reversed (i.e., to the Northeast Monsoon Current), with fresher BoB waters flowing westward toward the Arabian Sea (Figure 4b).

In boreal summer, some the EACC flow is diverted north into the northward flowing Somali Current, cutting off the supply of highly saline Arabian Sea waters from the EUC (Figures 4c and 4d). In these scenarios the strength of the EUC is irrelevant as there is less highly saline water available for it to transport eastward regardless.

7. Summarizing Remarks

The summer monsoon HSC in the BoB is the main source of salinity that balances the BoB's freshwater export (Vinayachandran et al., 1999, 2013). The source of this salinity has been linked to the ASHSW, which forms in the northern Arabian Sea, and is presumed to enter the BoB via the eastern Arabian Sea and the SMC (Jensen, 2001; Jensen et al., 2016; Schott & McCreary, 2001; Vinayachandran et al., 1999). In this study a new paradigm is presented to explain the origins and variability of the BoB HSC, stating chiefly that (1)

the BoB HSC primarily originates from the western equatorial Indian Ocean, and in particular, the western Arabian Sea is a key source region; (2) water mass pathways rather than transformation are key source of changes in the HSC; (3) the key pathways are dominated by the Somali Current, the EUC, and the SMC; (4) the anomalously saline BoB HSC is linked to an anomalously strong spring EUC; and (5) interannual variability in the EUC is shown to be dominated by zonal wind stress and ENSO. Given that the salinity stratification in the BoB is a crucial factor in the distribution (Shenoi et al., 2002) and variability (Li et al., 2016) of monsoon rainfall, our findings demonstrate a new oceanic mechanism through which ENSO and equatorial current dynamics will influence the rainfall of the South Asian monsoon.

Acknowledgments

The NERC Bay of Bengal Boundary Layer Experiment (BoBBLE) project supported A. S. F. and B. A. K. (NE/L013835/1) and B. G. M. W. and P. M. F. S. (NE/L013827/1). P. N. V., A. B., and C. P. N. are supported by the Indian BoBBLE program funded by the Ministry of Earth Sciences, Government of India, under its Monsoon Mission program administered by the Indian Institute of Tropical Meteorology, Pune. The authors would also like to acknowledge the Copernicus Marine Environment Monitoring Service for NEMO data access available online (<http://marine.copernicus.eu/services-portfolio/access-to-products/>), the International Argo Program for Argo data access (<http://argo.jcommops.org>), ESSO-INCOIS for TropFlux data access (<http://www.incois.gov.in/tropflux/>), the National Oceanic and Atmospheric Administration (NOAA) for ENSO data access (<http://www.cpc.ncep.noaa.gov/data/indices/>), and Dipole Mode Index data access (<https://stateoftheocean.osmc.noaa.gov/sur/ind/dmi.php>). The authors are also grateful for the helpful insight and comments from two anonymous reviewers.

References

- Antonov, J., Seidov, D., Boyer, T., Locarnini, R., Mishonov, A., Garcia, H., et al. (2010). World ocean atlas 2009. In S. Levitus (Ed.), *Salinity* (Vol. 2, pp. 184). Washington, DC: US Gov. Print. Off.
- Bonjean, F., & Lagerloef, G. S. (2002). Diagnostic model and analysis of the surface currents in the tropical Pacific Ocean. *Journal of Physical Oceanography*, *32*(10), 2938–2954.
- Boyer, T. P., Antonov, J. I., Baranova, O. K., Coleman, C., Garcia, H. E., Grodsky, A., et al. (2013). World ocean database 2013.
- Chatterjee, A., Shankar, D., Shenoi, S. S. C., Reddy, G. V., Michael, G. S., Ravichandran, M., et al. (2012). A new atlas of temperature and salinity for the North Indian Ocean. *Journal of Earth System Science*, *121*(3), 559–593.
- Chen, G., Han, W., Li, Y., Wang, D., & McPhaden, M. J. (2015). Seasonal-to-interannual time-scale dynamics of the equatorial undercurrent in the Indian Ocean. *Journal of Physical Oceanography*, *45*(6), 1532–1553.
- Desbruyeres, D., McDonagh, E. L., King, B. A., & Thierry, V. (2017). Global and full-depth ocean temperature trends during the early twenty-first century from argo and repeat hydrography. *Journal of Climate*, *30*(6), 1985–1997.
- Goswami, B. N. (2005). South Asian monsoon. In K. M. Lau & D. E. Waliser (Eds.), *Intraseasonal variability of the ocean and atmosphere* (pp. 19–61). Heidelberg: Springer.
- Jensen, T. G. (2001). Arabian sea and bay of bengal exchange of salt and tracers in an ocean model. *Geophysical Research Letters*, *28*(20), 3967–3970.
- Jensen, T. G. (2003). Cross-equatorial pathways of salt and tracers from the northern Indian Ocean: Modelling results. *Deep Sea Research Part II: Topical Studies in Oceanography*, *50*, 2111–2127.
- Jensen, T. G., Wijesekera, H. W., Nyadjro, E. S., Thoppil, P. G., Shriver, J. F., Sandeep, K. K., & Pant, V. (2016). Modeling salinity exchanges between the equatorial Indian Ocean and the Bay of Bengal. *Oceanography*, *29*(2), 92–101.
- Kindle, J. C., & Thompson, J. D. (1989). The 26- and 50-day oscillations in the western Indian Ocean: Model results. *Journal of Geophysical Research*, *94*(C4), 4721–4736.
- Knauss, J. A., & Taft, B. A. (1964). Equatorial undercurrent of the Indian Ocean. *Science*, *143*(3604), 354–356.
- Kumar, S. P., & Prasad, T. G. (1999). Formation and spreading of Arabian Sea high-salinity water mass. *Journal of Geophysical Research*, *104*(C1), 1455–1464.
- Kumar, B. P., Vialard, J., Lengaigne, M., Murty, V. S. N., & McPhaden, M. J. (2012). Tropflux: air-sea fluxes for the global tropical oceans-description and evaluation. *Climate Dynamics*, *38*(7-8), 1521–1543.
- Li, Y., Han, W., Wang, W., & Ravichandran, M. (2016). Intraseasonal variability of SST and precipitation in the Arabian Sea during the Indian Summer Monsoon: Impact of ocean mixed layer depth. *Journal of Climate*, *29*(21), 7889–7910.
- Madec, G. (2008). NEMO, the ocean engine, note du Pole de Modelisation, Institut Pierre-Simon Laplace (IPSL), France, no 27 ISSN no 1288-1619. Generic Tech. rep.
- Murty, V. S. N., Sarma, Y. V. B., Rao, D. P., & Murty, C. S. (1992). Water characteristics, mixing and circulation in the Bay of Bengal during southwest monsoon. *Journal of Marine Research*, *50*(2), 207–228.
- Nagura, M., & McPhaden, M. J. (2010). Wyrтки jet dynamics: Seasonal variability. *Journal of Geophysical Research*, *115*, C07009. <https://doi.org/10.1029/2009JC005922>
- Nagura, M., & McPhaden, M. J. (2016). Zonal propagation of near-surface zonal currents in relation to surface wind forcing in the equatorial Indian Ocean. *Journal of Physical Oceanography*, *46*(12), 3623–3638.
- Prasad, T. G., & Ikeda, M. (2002). A numerical study of the seasonal variability of Arabian Sea high-salinity water. *Journal of Geophysical Research*, *107*(C11), 3197. <https://doi.org/10.1029/2001JC001139>
- Reppin, J., Schott, F. A., Fischer, J., & Quadfasel, D. (1999). Equatorial currents and transports in the upper central Indian Ocean: Annual cycle and interannual variability. *Journal of Geophysical Research*, *104*(C7), 15,495–15,514.
- Reverdin, G. (1987). The upper equatorial Indian Ocean. The climatological seasonal cycle. *Journal of Physical Oceanography*, *17*(7), 903–927.
- Reynolds, R. W., Rayner, N. A., Smith, T. M., Stokes, D. C., & Wang, W. (2002). An improved in situ and satellite SST analysis for Climate. *Journal of climate*, *15*(13), 1609–1625.
- Saji, N. H., Goswami, B. N., Vinayachandran, P. N., & Yamagata, T. (1999). A dipole mode in the tropical Indian Ocean. *Nature*, *401*(6751), 360.
- Sanchez-Franks, A., Kent, E. C., Matthews, A. J., Webber, B. G. M., Peatman, S. C., & Vinayachandran, P. N. (2018). Intraseasonal variability of air-sea fluxes over the Bay of Bengal during the southwest monsoon. *Journal of Climate*, *31*, 7087–7109.
- Schott, F. A., & McCreary, J. P. Jr (2001). The monsoon circulation of the Indian Ocean. *Progress in Oceanography*, *51*(1), 1–123.
- Schott, F. A., Xie, S. P., & McCreary, J. P. (2009). Indian ocean circulation and climate variability. *Reviews of Geophysics*, *47*, RG1002. <https://doi.org/10.1029/2007RG000245>
- Shankar, D., Vinayachandran, P. N., & Unnikrishnan, A. S. (2002). The monsoon currents in the north Indian Ocean. *Progress in Oceanography*, *52*(1), 63–120.
- Shenoi, S. S. C., Shankar, D., & Shetye, S. R. (2002). Differences in heat budgets of the near-surface Arabian Sea and Bay of Bengal: Implications for the summer monsoon. *Journal of Geophysical Research*, *107*(C6), 3052. <https://doi.org/10.1029/2000JC000679>
- Shenoi, S. S. C., Shetye, S. R., Gouveia, A. D., & Michael, G. S. (1993). *Salinity extrema in the Arabian Sea*. Germany: Mitt. Geol. Palaontol University of Hamburg.
- Shetye, S. R., Gouveia, A. D., Shankar, D., Shenoi, S. S. C., Vinayachandran, P. N., Sundar, D., et al. (1996). Hydrography and circulation in the western Bay of Bengal during the northeast monsoon. *Journal of Geophysical Research*, *101*(C6), 14,011–14,025.

- Vinayachandran, P. N., Masumoto, Y., Mikawa, T., & Yamagata, T. (1999). Intrusion of the southwest monsoon current into the Bay of Bengal. *Journal of Geophysical Research*, *104*(C5), 11,077–11,085.
- Vinayachandran, P. N., Matthews, A. J., Vijay Kumar, K., Sanchez-Franks, A., Thushara, V., George, J., et al. (2018). Bobble (bay of bengal boundary layer experiment): Ocean-atmosphere interaction and its impact on the south Asian monsoon. *Bulletin of the American Meteorological Society*, *99*, 1569–1587.
- Vinayachandran, P. N., Murty, V. S. N., & Ramesh Babu, V. (2002). Observations of barrier layer formation in the Bay of Bengal during summer monsoon. *Journal of Geophysical Research*, *107*(C12), 8018. <https://doi.org/10.1029/2001JC000831>
- Vinayachandran, P. N., Shankar, D., Vernekar, S., Sandeep, K. K., Amol, P., Neema, C. P., & Chatterjee, A. (2013). A summer monsoon pump to keep the Bay of Bengal salty. *Geophysical Research Letters*, *40*, 1777–1782. <https://doi.org/10.1002/grl.50274>
- Webber, B. G. M., Matthews, A. J., Vinayachandran, P. N., Neema, C. P., Sanchez-Franks, A., Vijith, V., et al. (2018). The dynamics of the southwest monsoon current in 2016 from high-resolution in situ observations and models. *Journal of Physical Oceanography*, *48*(10), 2259–2282. <https://doi.org/10.1175/JPO-D-17-0215.1>
- Wyrtki, K. (1973). An equatorial jet in the Indian Ocean. *Science*, *181*(4096), 262–264.
- Yamagata, T., Behera, S. K., Luo, J.-J., Masson, S., Jury, M. R., & Rao, S. A. (2004). Coupled ocean-atmosphere variability in the tropical Indian Ocean. *Earth Climate: The Ocean Atmosphere Interaction, Geophysical Monograph*, *147*, 189–212.
- Yu, W., Xiang, B., Liu, L., & Liu, N. (2005). Understanding the origins of interannual thermocline variations in the tropical Indian Ocean. *Geophysical Research Letters*, *32*, L24706. <https://doi.org/10.1029/2005GL024327>
- Zhang, D., McPhaden, M. J., & Lee, T. (2014). Observed interannual variability of zonal currents in the equatorial Indian Ocean thermocline and their relation to Indian Ocean Dipole. *Geophysical Research Letters*, *41*, 7933–7941. <https://doi.org/10.1002/2014GL061449>